International Journal of Pharmaceutics 430 (2012) 129–140

Contents lists available at SciVerse ScienceDirect

International Journal of Pharmaceutics

journal homepage: www.elsevier.com/locate/ijpharm

Novel nanostructural photosensitizers for photodynamic therapy: *In vitro* studies

Kinga Nawalany[a,b,1], Aleksandra Rusin[c,1], Mariusz Kepczynski[a], Piotr Filipczak[c], Marta Kumorek[a], Bartłomiej Kozik[a], Hana Weitman[d], Benjamin Ehrenberg[d], Zdzisław Krawczyk[c,e], Maria Nowakowska[a,*]

[a] *Faculty of Chemistry, Jagiellonian University, Ingardena 3, 30-060 Kraków, Poland*
[b] *Faculty of Commodity Science, Cracow University of Economics, Rakowicka 27, 31-510 Kraków, Poland*
[c] *Maria Sklodowska-Curie Memorial Cancer Center and Institute of Oncology, Gliwice Branch, Wybrzeże Armii Krajowej 15, 44-100 Gliwice, Poland*
[d] *Department of Physics, Bar Ilan University, Ramat Gan 52900, Israel*
[e] *Department of Organic Chemistry, Bioorganic Chemistry and Biotechnology, Silesian University of Technology, Akademicka 2A, 44-100 Gliwice, Poland*

ARTICLE INFO

Article history:
Received 7 December 2011
Received in revised form 16 March 2012
Accepted 5 April 2012
Available online 15 April 2012

Keywords:
Porphyrin
Pegylation
PDT
Phototoxicity
Colocalization
Liposomes

ABSTRACT

Photosensitizing properties of 5,10,15,20-tetrakis(4-hydroxyphenyl)porphyrin (p-THPP) functionalized by covalent attachment of one chain of poly(ethylene glycol) (PEG) with a molecular weight of 350, 2000, or 5000 Da (p-THPP-PEG_{350}, p-THPP-PEG_{2000}, p-THPP-PEG_{5000}) were studied *in vitro*. Dark and photo cytotoxicity of these photosensitizers delivered in solution or embedded in liposomes were evaluated on two cell lines: a human colorectal carcinoma cell line (HCT 116) and a prostate cancer cell line (DU 145), and compared with these treated with free p-THPP. The attachment of PEG chains results in the pronounced reduction of the dark cytotoxicity of the parent porphyrin. Cell viability tests have demonstrated that the phototoxicity of pegylated porphyrins is dependent on the length of PEG chain and p-THPP-PEG_{2000} exhibited the highest photodynamic efficacy for both cell lines. The encapsulation into liposomes did not improve the PDT effect. However, the liposomal formulation of p-THPP-PEG_{2000} showed a greater tendency to induce apoptosis in both cell lines than the parent or pegylated porphyrin delivered in solution. The colocalization of p-THPP, p-THPP-PEG_{2000} and p-THPP-PEG_{2000} enclosed in liposomes with fluorescent markers for lysosomes, mitochondria, endoplasmatic reticulum (ER) and Golgi apparatus (GA) was determined in the HCT 116 line. The p-THPP exhibited ubiquitous intracellular distribution with a preference for membranes: mitochondria, ER, GA, lysosomes and plasma membrane. Fluorescence of p-THPP-PEG_{2000} was observed within the cytoplasm, with a stronger signal detected in membranous organelle: mitochondria, ER, GA and lysosomes. In contrast, p-THPP-PEG_{2000} delivered in liposomes gave a distinct lysosomal pattern of localization.

1. Introduction

Photodynamic therapy (PDT) is currently used as a popular form of photochemotherapy for a wide variety of clinical applications (Allison and Sibata, 2010; Juzeniene et al., 2007). This treatment requires the presence of a drug, called photosensitizer, activating light of a specific wavelength and molecular oxygen to produce a localized damage in tumor tissues and/or their vasculature (Henderson and Dougherty, 1992; Moan and Peng, 2003). In a clinical context the term PDT implies a therapeutic effect,

Abbreviations: Bodipy-Fl, 4,4-difluoro-5,7-dimethyl-4-bora-3a,4a-diaza-*s*-indacene-3-propionic acid; DAPI, 4′-6′-diamidino-2-phenylindole; DiOC6, 3-hexyl-2-[3-(3-hexyl-2(3*H*)benzoxazolylidene)-1-propenyl]benzoxazolium iodide; DMA, 9,10-dimethylanthracene; DMEM, Dulbecco's modified eagle medium; DMSO, dimethyl sulfoxide; DU 145, human prostate adenocarcinoma cell line; EDTA, 2,2′,2″,2‴-(ethane-1,2-diyldinitrilo)tetraacetic acid; ER, endoplasmic reticulum; FBS, fetal bovine serum; GA, Golgi apparatus; HCT 116, human colon adenocarcinoma cell line; IC_{50}, half maximal inhibitory concentration; m-THPC, 5,10,15,20-tetra(m-hydroxyphenyl)chlorin; MTS, 3-(4,5-dimethylthiazol-2-yl)-5-(3-carboxymethoxyphenyl)-2-(4-sulfophenyl)-2H-tetrazolium); MW, molecular weight; PBS, phosphate buffered saline; PC, L-α-phosphatidylcholine; PDT, photodynamic therapy; PEG, poly(ethylene glycol); PS, photosensitizer; p-THPP, 5,10,15,20-tetrakis(4-hydroxyphenyl)porphyrin; p-THPP-PEG_{350}, 5,10,15,20-tetrakis(4-hydroxyphenyl)porphyrin modified with poly(ethylene glycol) of molecular weight 350 Da; p-THPP-PEG_{2000}, 5,10,15,20-tetrakis(4-hydroxyphenyl)porphyrin modified with poly(ethylene glycol) of molecular weight 2000 Da; p-THPP-PEG_{5000}, 5,10,15,20-tetrakis(4-hydroxyphenyl)porphyrin modified with poly(ethylene glycol) of molecular weight 5000 Da; RPMI, Roswell Park Memorial Institute medium; SSL, sterically stabilized liposomes; SUV, small unilamellar vesicle; TTR, tumor to normal tissue ratio; $^1O_2$, singlet oxygen.

* Corresponding author. Tel.: +48 12 663 2250; fax: +48 12 634 0515.
E-mail address: nowakows@chemia.uj.edu.pl (M. Nowakowska).

[1] Both authors contributed equally to the experimental work.

0378-5173/$ – see front matter © 2012 Elsevier B.V. All rights reserved.
http://dx.doi.org/10.1016/j.ijpharm.2012.04.016

while in cell culture models the term PDT indicates the lethal effects of light irradiation on dye-sensitized cells. At the cellular level, unrepairable damage to mitochondria, endoplasmic reticulum, and lysosomes, caused by singlet oxygen and/or other reactive oxygen species (formed as a result of quenching of electronically excited molecules of photosensitizer by molecular oxygen) leads to necrotic or apoptotic cell death, depending on the cell type, the photosensitizer, its subcellular localization and treatment protocol (Buytaert et al., 2007; Dellinger, 1996; Mroz et al., 2011; Wyld et al., 2001). Apoptosis, in contrast to necrosis, is considered to be a programmed form of cell death, which occurs under normal physiological conditions and activates cells in its own demise without inflammatory response. Apoptosis may be executed by various mechanisms as a result of primary damage caused by accumulated photosensitizers in different organelles (Oleinick et al., 2002). The mitochondria targeting drugs cause the loss of mitochondrial membrane potential and cytochrome c release (Morgan and Oseroff, 2001). The lysosomes targeting sensitizers cause membrane disruption and cathepsins release (Ichinose et al., 2006). The endoplasmic reticulum (ER) targeting drugs induce the so-called ER stress and elevated intracellular calcium level (He et al., 2010), all of which are proapoptotic signals (Ball et al., 1998).

Many efforts have been undertaken to develop new photosensitizing agents with a high efficacy for photodynamic treatment of cancer and some other diseases (Berlanda et al., 2010; Mroz et al., 2007). Porphyrins and their derivatives, absorbing light in the visible spectral region, are studied as potential first or second-generation sensitizers because of their high anti-cancer efficiency (Peng et al., 2010). The factors limiting the use of porphyrins in PDT are their poor solubility in water, low chemical purity and high dark toxicity. The incorporation of photosensitizers into various nano-carriers, including lipid vesicle carriers (Chen et al., 2005), polymeric formulations (Deda et al., 2009; Konan et al., 2003a,b; Vargas et al., 2004) and silica nanoparticles (Roy et al., 2003; Zhao et al., 2009) is a popular strategy to overcome those limitations.

The attachment of drugs to poly(ethylene glycol) (PEG), a hydrophilic and biocompatible polymer, is a highly effective method to improve their solubility in water, but also to protect them against their aggregation in aqueous media, to decrease their cytotoxicity, and to bolster selectivity for cancer cells (Hamblin et al., 2001; Lottner et al., 2002; Sibrian-Vazquez et al., 2007). Hematoporphyrin or tetraarylporphyrin-platinum (II) complexes with two or three PEG fragments bounded to a porphyrin core were proposed as potential photosensitizers for PDT by Lottner et al. (2002). Grahn et al. (1999) studied the biological activity of the four 5,10,15,20-tetra(m-hydroxyphenyl)chlorin (m-THPC-PEG) conjugates and proved their high *in vivo* activities.

It is known that selective therapeutic effect against tumor cells and tissues can be provided not only by the nature of the drugs or tumor physiology but also by using effective delivery systems. One of the strategies for enhancing PDT efficacy is based on the formulation of lipid carriers for photosensitizing agents. Liposomes can be used to enhance their clinical effects, to reduce their toxicity and to protect them from metabolism and immune responses. Liposomal formulations of photosensitizing drugs may help to achieve better selectivity for tumor tissue (Derycke and de Wittle, 2004).

In the previous paper (Nawalany et al., 2009) we investigated the photodynamic efficacy of two photosensitizing systems: p-THPP encapsulated in sterically stabilized liposomes (SSL) and p-THPP functionalized with one or two PEG_{2000} chains and dissolved in buffer. The dark and photo cytotoxicity of these systems were evaluated in two cell lines: HCT 116, a human colon adenocarcinoma cell line, and DU 145, a prostate cancer cell line, and compared with these determined for the pure p-THPP. The *in vitro* studies revealed that both encapsulation in liposomes and attachment of PEG chains had a pronounced impact on the reduction of dark cytotoxicity of the parent porphyrin. Moreover, the SSL liposomes loaded with p-THPP were more readily taken up by the cells and showed a higher photocytotoxicity towards both cell lines used in the studies than the pegylated porphyrin dissolved in a culture medium. However, a photosensitizer should preferentially accumulate in the malignant tissue after its administration. The ability to localize preferentially in malignant tissue is commonly expressed as a tumor to normal tissue ratio (TTR) (Hornung et al., 1999). It was demonstrated in *in vivo* study that pegylation significantly increases the value of TTR ratio for a given photosensitizer (Hornung et al., 1999; Westermann et al., 1998). Therefore, we decided to continue the studies of the PEG-formulation/activity relationships and the photodynamic efficacy of porphyrin-based photosensitizers.

This paper presents the results of our *in vitro* studies on the development of the efficient nanoformulations of porphyrin for PDT. For the first time, the effect of the PEG chain length on the photodynamic activity of the series of PEG-functionalized tetraarylporphyrin was carefully evaluated. The process of liposome encapsulation of pegylated systems was successfully carried out and the efficacy of liposomal formulation *in vitro* was also studied. Dark and photo cytotoxicity of these photosensitizers were evaluated on two cell lines: HCT 116 and DU 145 and compared with these treated with free p-THPP and p-THPP encapsulated into SSL liposomes. It is well known that the sub-cellular localization of photosensitizers may govern much of the signaling and may determine the mode of cell death, which is induced by PDT treatment. For that reason, the kinetics of cellular uptake and the intracellular co-localization of p-THPP-PEG_{2000} formulations (which exhibit the most significant photodynamic activity) were carefully evaluated by means of flow cytometric analysis and confocal laser scanning microscopy with the application of properly chosen fluorescence markers. Additionally, the time course and the mechanism of cell death after PDT were determined.

2. Material and methods

2.1. Synthesis of the pegylated porphyrins

Three PEG-functionalized porphyrins (p-THPP-PEG_{350}, p-THPP-PEG_{2000} and p-THPP-PEG_{5000}) were synthesized by covalent attachment of PEG chains of various molecular weights (350, 2000 and 5000 Da) to commercially available 5,10,15,20-tetrakis(4-hydroxyphenyl)porphyrin (p-THPP, Sigma–Aldrich). The procedures of the synthesis were described in our previous paper (Nawalany et al., 2008).

Stock solutions of p-THPP and p-THPP-PEG_{350} were prepared in DMSO (Aldrich Chemical Co., Milwaukee, WI). The p-THPP-PEG_{2000} and p-THPP-PEG_{5000} in all experiments were supplied as phosphate-buffered saline (PBS) solutions at pH 7.4. The stock solutions were next diluted in a cell growth medium to final concentrations. All solutions were handled in the dark to avoid photobleaching.

2.2. Encapsulation in liposomes

L-α-Phosphatidylcholine (PC) type XIII-E from egg yolk (99%, solution of 100 mg/mL in ethanol) was obtained from Sigma Chemical Co. (St. Louis, MO) and used to prepare liposomes. It was a mixture of lipids with the following fatty acid makeup: 33% C16:0 (palmitic), 13% C18:0 (stearic), 31% C18:1 (oleic), and 15% C18:2 (linoleic) (other fatty acids being minor contributors), which gives an average molecular weight of approximately 768 g/mol. The liposome dispersions with incorporated pegylated porphyrins were prepared by extrusion. The adequate amount of pegylated porphyrin was placed in a volumetric flask and mixed with 200 μL of

the lipid solution. Then, the ethanol was gently evaporated under the flow of nitrogen to form a thin film. The dry film was redissolved in diethyl ether which was reevaporated under nitrogen to complete dryness. A 10 mM PBS buffer was added till a lipid concentration of 10 mg/mL was attained. The sample was sonicated for 5 min at 20 °C in a Bronsonic ultrasonic bath. The obtained multilamellar liposome suspension was subjected to five freeze-pump-thaw cycles from liquid nitrogen temperature to 60 °C. Next, small unilamellar liposomes (SUV) were formed by extrusion 10 times through two stacked membrane filters with 200-nm pores (Nucleopore Track-Etch Membrane Whatman filters) using the PPH Marker manual extruder, and 15 times through membrane filters with 100 nm pores. The liposome dispersions were stored at 4 °C.

In the case of singlet oxygen quantum yield measurements SUV were formed by sonication using a probe sonicator (MSE Soniprep 150, UK). Next the liposomes were incubated for 24 h with an appropriate amount of DMA in the dark.

2.3. Determination of singlet oxygen quantum yields in methanol and in liposome

Quantum yields of singlet oxygen generation (Φ_Δ) were measured indirectly relative to hematoporphyrin IX or Rose Bengal (Roslaniec et al., 2000). 9,10-Dimethylanthracene (DMA, Sigma–Aldrich) was employed as a singlet oxygen trap, since it reacts rapidly and selectively with singlet oxygen in many organic solvents forming non-fluorescent 9,10-endoperoxide. The reaction mixture consisted of methanol or the liposome dispersion, sensitizer (5 μM) and DMA (5 μM) was air saturated and stirred magnetically during the measurement to obtain uniform irradiation of the whole sample contents. We performed *in situ* fluorescence measurements of DMA in a time-driven mode, while the laser beam (Coherent Innova 200 Ar^+ laser at 514.5 nm, 30–50 mW) transverse the sample cuvette along its long axis, at 90° to the direction of the excitation and emission channels of the fluorimeter, in which the cuvette was placed. The constancy of the laser power during the experiments was verified at the sample surface with a power meter (model PD2-A, Ophir, Jerusalem, Israel). The rate of photon absorption, k_{pho}, was calculated using Eq. (1):

$$k_{pho} = \frac{0.98 \cdot P \cdot (1 - 10^{(-abs \cdot L)})}{E \cdot V} \quad (1)$$

where P is the laser power in mW, *abs* is the optical density per centimeter at the laser wavelength, L is the sample length along the laser beam axis, E is the number of Einstein units (1 Einstein = 6.023×10^{23} photons) per second per watt of light and V is the volume of the sample (in mL). The factor 0.98 corrects the light reflected at the air/sample interface, using the Fresnel equation.

The DMA fluorescence disappearance followed first-order decay kinetics according to the following Eq. (2):

$$DMA_{flu} = A \exp^{-k_{DMA} \cdot t} \quad (2)$$

where k_{DMA} is the rate constant for the decrease of DMA fluorescence, DMA_{flu}; t is the time. For each sensitizer, the single oxygen quantum yield is proportional to the value of (k_{DMA}/k_{pho}). If $\Phi_{\Delta,stand}$ of a standard sensitizer is known (in a particular solvent), $\Phi_{\Delta,sens}$ can be determined, in the same solvent, using the following expression (3):

$$\frac{\Phi_{\Delta,sens}}{\Phi_{\Delta,stand}} = \frac{(k_{DMA}/k_{pho})_{sens}}{(k_{DMA}/k_{pho})_{stand}} \quad (3)$$

Rose Bengal was used as a standard for the organic measurements, and hematoporphyrin IX was used as a standard for membrane measurements.

2.4. Cellular uptake

A human colon adenocarcinoma cell line (HCT 116) and a prostate adenocarcinoma cell line (DU 145) were obtained from the American Type Culture Collection and maintained in the Cancer Center and the Institute of Oncology in Gliwice (Poland). The cells were grown as a monolayer in RPMI 1640 culture medium (Sigma–Aldrich) supplemented with 10% fetal bovine serum (ICN, UK) and 40 μg/mL gentamicin sulfate (Sigma–Aldrich, Germany) at 37 °C, 95% humidity and 5% CO_2.

Confocal laser scanning microscopy (CLSM) was used to visualize the intracellular accumulation of the photosensitizing systems. Cells were seeded on NUNC thin glass 4-well plates at the density of 10,000 cells per well and left for 24 h for adhesion to the bottom. The growth medium was replaced with a medium containing different photosensitizer systems of equivalent concentration of porphyrin dye (10 μg/mL). The cells were incubated for 3.5 h at 37 °C. Afterwards, the cells were washed twice with PBS buffer and examined under the confocal microscope (Nikon).

Kinetics of intracellular accumulation of different photosensitizing systems was examined using a FACScanto™ flow cytometer (Becton Dickinson, Mountain View, CA) equipped with a 15-mW 488 nm air-cooled argon ion laser, 655 nm long-pass mirror, and 670 nm long-pass filter. Cells were seeded in 24-well plates (Nunc) at a density of 20,000 cells per well and left for 24 h. Next, the cells were incubated with porphyrins (10 μg/mL) for 45 min, 2, 3, 4, and 6 h, harvested by trypsin–EDTA, and washed with PBS. The intensity of fluorescence was measured immediately. At least 10,000 events were analyzed. The level of autofluorescence was measured in untreated cells. Data represent the means of two independent experiments.

2.5. PDT treatment and cell viability test

HCT 116 and DU 145 cells were seeded on 3 cm plates (NUNC) at the density of 1.33×10^5 cells per plate and left for 24 h to allow them to adhere to the bottom. The cells were incubated for 4 h with different concentration of porphyrins: 1, 2.5, 5, 10, and 20 μg/mL. Then the medium containing porphyrins was replaced with phenol red free medium and plates were exposed to the red light source (a halogen lamp 1000 W, with heat isolation filter and 610 nm long-pass filters) for 2.5 min (15 J/cm^2). Control cells were neither treated with porphyrins nor irradiated with red light. Dark control cells were treated with porphyrins exactly as described for PDT, except for irradiation with red light, and light control cells were exposed to red light without prior incubation with porphyrins. All experiments were performed in triplicates.

The cell viability test, MTS CellTiter 96® (Promega), was performed 24 h after PDT following a standard protocol. In brief, the medium in culture plates was replaced with MTS in DMEM without phenol red, and cells were incubated for 4 h at 37 °C. The solution was transferred to the well in 96-well culture plate (Nunc, Denmark). Optical density was determined at 490 nm using a microplate reader (BioTek Instruments, USA). The viability was expressed as a percentage of control. IC_{50} was defined as a concentration of a drug that decreases cell viability by 50%.

2.6. Time course of cell death

Time course of cell death after PDT was studied for HCT 116 and DU 145 cells treated with three photosensitizer systems: (i) p-THPP in DMSO, (ii) p-THPP-PEG_{2000} in PBS and (iii) p-THPP-PEG_{2000} incorporated into liposomes. The integrity of plasma membrane was checked with propidium iodide exclusion assay 3, 6, and 24 h after the PDT treatment. Floating cells were collected and pooled with adherent cells, detached with 0.25% trypsin/EDTA. After wash

with PBS the cells were stained with 1 μg/mL propidium iodide for 10 min at room temperature. The cells were analyzed with the flow cytometer. The fluorescence emission was acquired in log mode. At least 10,000 events were analyzed. Control cells (treated neither with photosensitizer nor with light), stained with propidium iodide were used to determine the fluorescence intensity level of the population of living cells. The cells with stronger fluorescence were regarded as permeable for propidium iodide, thus dying or dead. The data represent the averages of three independent experiments.

2.7. Examination of cellular and nuclear morphology after PDT

Cells were assessed for changes in their morphology, 24 h after PDT in their culture dishes, under an OLYMPUS IX80 inverted microscope equipped with differential interference contrast (DIC). To assess the morphology of nuclei the cells were collected, 24 h after PDT. Floating cells were pooled with adherent cells, detached with 0.25% trypsin/EDTA. After washing with PBS, the cells were cytospinned, fixed with methanol, stained with DAPI (300 nM in PBS) and mounted with DAKO fluorescence mounting medium. The specimens were observed under a NIKON Eclipse fluorescence microscope and images were taken with a Hamamatsu C5810 camera. Index of cells with apoptotic morphology was counted in at least 500 cells/treatment. Experiments were repeated three times.

2.8. Colocalization of porphyrins with probes for lysosomes, mitochondria, Golgi apparatus and endoplasmatic reticulum

To gain information about the subcellular localization of the red fluorescence photosensitizers delivered to the HCT 116 cells, we used a colocalization technique with fluorescent markers. Lysotracker green (Molecular Probes) was used for the detection of lysosomes, mitotracker green (Molecular Probes) was used for the detection of mitochondria, endoplasmic reticulum was stained with DiOC6 (Molecular Probes) and Golgi apparatus – with Bodipy-Fl ceramide (Molecular Probes). Cells were seeded in thin bottom glass 8-chamber slides (Nunc) at a density of 10,000 cells/per well and left for 24 h. After the incubation for 4 h with different photosensitizer systems (5 μg/mL p-THPP, 10 μg/mL p-THPP-PEG_{2000}, and 20 μg/mL p-THPP-PEG_{2000} in liposomes), lysotracker green (100 nM) and mitotracker green (200 nM) were added and the incubation was continued for the time indicated by the marker manufacturers (30 min for lysotracker and 5 min for mitotracker). We observed a detrimental effect of DiOC6 on HCT 116 cells, manifested by mitochondrial swelling and plasma membrane blebbing, even when cells were observed immediately after the addition of this marker, which disqualified this agent for live cell imaging. For the proper intracellular localization of porphyrins the cells were fixed shortly with 4% paraformaldehyde (5 min), which allowed to retain fluorescent signal. The fixation was also performed after staining of Golgi apparatus with Bodipy-Fl ceramide in order not to change the localization of a probe in consequence of membrane trafficking.

Cells were analyzed with a A1-Si Nikon Inc. (Japan) confocal laser scanning system built onto a Nikon inverted microscope T*i*-E using a Plan Apo 100×/1.4 Oil DIC objective. Images were acquired at a resolution of 2048 × 2048. The A1-Si system was equipped with a four-channel detection as well as LSBF imaging by diascopic detection of forward scattered excitation laser light during confocal laser scanning. The excitation for confocal microscopy was provided by a set of four diode lasers with excitation wavelengths at 405, 488, 561, and 638 nm.

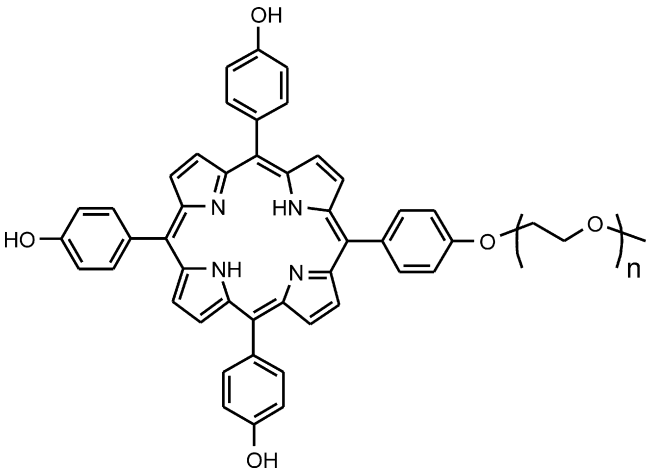

Fig. 1. Chemical structure of 5,10,15,20-tetrakis(4-hydroxyphenyl)porphyrin (p-THPP) with attached PEG chain.

3. Results and discussion

3.1. Characterization of the photosensitizer systems

The aim of the studies presented in this paper was to investigate the effect of covalent attachment of one PEG chain with different length on the *in vitro* PDT activity of 5,10,15,20-tetrakis(4-hydroxyphenyl)porphyrin (p-THPP). Three PEG-functionalized porphyrins (p-THPP-PEG_{350}, p-THPP-PEG_{2000} and p-THPP-PEG_{5000}) were synthesized using the procedure reported earlier (Nawalany et al., 2008). The chemical structures of the studied compounds are presented in Fig. 1.

Quantum yield of singlet oxygen generation (Φ_Δ) is an important measure of photosensitization efficiency. The values of Φ_Δ for p-THPP and p-THPP-PEG_{2000} in methanol and in liposome suspension media are summarized in Table 1. The absolute yields were calculated by the comparison of the rate of DMA photodestruction by the free and pegylated p-THPP with that obtained by standard sensitizers like Rose Bengal or hematoporphyrin, in methanol and in lecithin liposomes, respectively.

As can be seen from the data presented in Table 1, the parent p-THPP and its pegylated derivative show comparable values of Φ_Δ in methanol solution. The value for p-THPP is somewhat lower than the value obtained for the same compound, by Bonnett et al. (1988) who quoted a value of $\Phi_\Delta = 0.56$ in methanol. However, these results are in line with earlier results obtained for other efficient porphyrin photosensitizers. Quantum yields of singlet oxygen production by m-THPP and m-THPC in methanol are found to be 0.46 and 0.43, respectively (Bonnett, 1995). Although the values of Φ_Δ are considerably higher for liposomal systems of both, p-THPP and p-THPP-PEG_{2000} photosensitizers, a real change is observed for p-THPP-PEG_{2000}. The value of quantum yield of singlet oxygen formation in that hybrid system reaches almost 1 within the experimental error.

Table 1
Experimentally measured singlet oxygen yields (Φ_Δ) of photosensitizers dissolved in methanol or incorporated into liposomal membrane.

Photosensitizing system	Φ_Δ in methanol	Φ_Δ in liposomes
p-THPP	0.33 ± 0.03	0.42 ± 0.03
p-THPP-PEG_{2000}	0.36 ± 0.06	0.91 ± 0.07

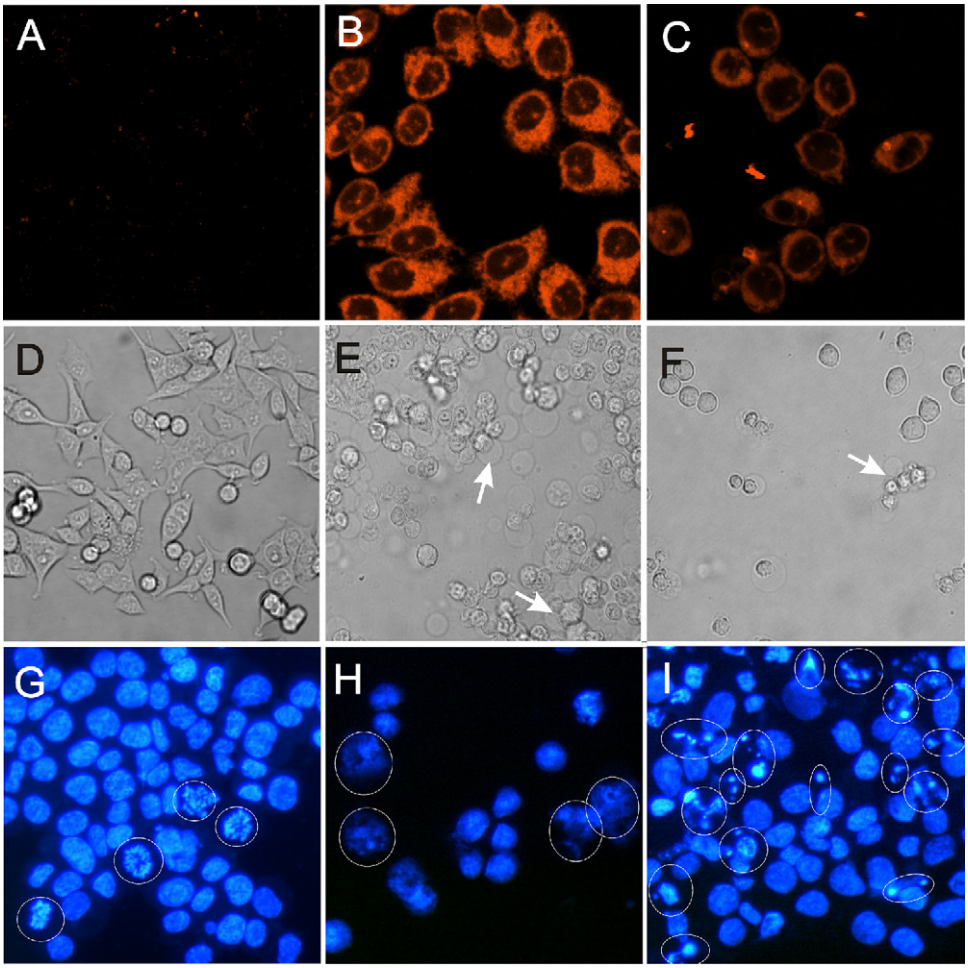

Fig. 2. (A–C) Confocal images of HCT 116 cells after 3.5 h incubation with different forms of p-THPP-PEG_{2000}. (A) Unlabeled control showing no fluorescence, (B) 10 μg/mL p-THPP-PEG_{2000} in PBS, (C) 10 μg/mL p-THPP-PEG_{2000} enclosed in liposomes, (D–F) cellular morphology of HCT 116 cells 24 h after PDT. (D) Control cells (irradiated with light without pretreatment with a photosensitizer). (E) PDT with 5 μg/mL of p-THPP-PEG_{2000} (arrows – damaged cells with poured out contents), (F) PDT with p-THPP-PEG_{2000} enclosed in liposomes (arrows – shrinked cells). (G – H) Nuclear morphology of HCT 116 cells 24 h after PDT. (G) Control cells (irradiated with light without pretreatment with a photosensitizer; circles – mitosis), (H) PDT with 5 μg/mL of p-THPP-PEG_{2000}, (circles – nuclear swelling), (I) PDT with p-THPP-PEG_{2000} enclosed in liposomes (circles – fragmented nuclei characteristic for apoptosis).

3.2. Cellular uptake of photosensitizing systems

Cellular uptakes of different photosensitizing systems were evaluated using a colon cancer cell line HCT 116 and a prostate cancer cell line DU 145. The cellular uptake was initially visualized using CLSM microscopy. Fig. 2B and C shows as examples confocal images of HCT 116 cells treated with p-THPP-PEG_{2000} in buffer and enclosed in liposomes. The pegylated porphyrins dissolved in a culture medium were taken up by cells, which were observed as intracellular fluorescence under the microscope. Encapsulation of p-THPP-PEG_{2000} into liposomes markedly reduced the uptake (Fig. 2C).

To gain more quantitative information, the uptake kinetics of different photosensitizing systems by HCT 116 and DU 145 cells was measured with a flow cytometer. The changes in fluorescence intensity were shown in Fig. 3. The most intensive accumulation was observed for unmodified p-THPP in both the tested cell lines (data not shown). The intensity of uptake of pegylated porphyrins by both cell lines increased in a series: p-THPP-PEG_{350} < p-THPP-PEG_{5000} < p-THPP-PEG_{2000}. Liposomal formulation significantly decreased the cellular uptake of p-THPP-PEG_{2000} and p-THPP-PEG_{5000}. However, the enhancement of uptake was observed for liposomal formulation of p-THPP modified with PEG_{350}. Additionally, it was observed for HCT 116 cell line that cellular uptake of p-THPP-PEG_{350} and liposomal formulation of p-THPP-PEG_{2000} and p-THPP-PEG_{5000} reached a plateau after 4 h (Fig. 3A). In the case of the rest of photosensitizers the fluorescence intensity increased with incubation time up to 6 h. Considering results obtained for DU 145 cell line (Fig. 3B), it was found that the uptake of p-THPP-PEG_{2000} in PBS and liposomal formulations of p-THPP-PEG_{350} and p-THPP-PEG_{5000} increased up to 4 h and saturated thereafter, while the accumulation of the other photosensitizers steadily increased with time. Comparing the results obtained for that two cell lines, it is clearly visible that the accumulation of dyes in DU 145 cells was definitely less efficient than in the HCT 116 cells. It suggests that the DU 145 cells were more resistant to treatment with photosensitizers.

The flow cytometric analysis showed that the attachment of PEG to the porphyrin core as well as polymer chain length had an impact on the kinetics of intracellular accumulation. These results were partially consistent with our previous studies on interactions between the pegylated porphyrins and the phospholipid bilayer used as a model membrane (Nawalany et al., 2008). We showed that the attachment of PEG chain to the p-THPP ring caused the reduction of the partitioning of the chromophore to the liposomal membrane. It was explained by the effect of PEG on the changes of the polarity of aqueous phase and distribution of porphyrin chromophore

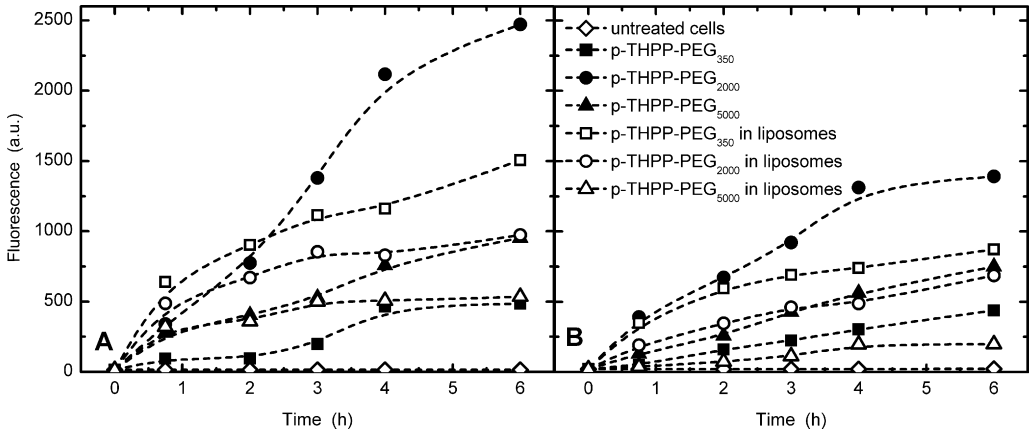

Fig. 3. Time-dependent uptake of the photosensitizing systems (10 μg/mL) by a human colon adenocarcinoma cells HCT 116 (A) and a prostate adenocarcinoma cells DU 145 (B).

between the lipid membrane and water phase. However, the affinity of porphyrin to lipid phase was found to be weakly dependent on the molecular weight of the attached PEG. The binding constant of pegylated porphyrins slightly decreased with the increased of polymer chain length. On the other hand, studies of PEG behavior in aqueous solution indicated that PEG chain has an ability to associate the water molecules, which results in a significant increase of its size (Roberts et al., 2002). It was calculated that one ethylene oxide unit can bind approximately 2 or 3 water molecules. Therefore, the observed slower uptake of p-THPP-PEG_{5000} by cellular membrane compared to p-THPP-PEG_{2000} might have been caused by the formation of water-PEG large clusters under physiological condition. Another possible explanation of the reduced tendency of p-THPP-PEG_{5000} to permeate through the cellular membrane lies in the polarity of this conjugation. As was reported in the literature, the lipophilicity of the photosensitizers can influence the cellular uptake and biological activity of the drug (Henderson et al., 1997). Thus, the conjugation of p-THPP with PEG of molecular weight 5000 Da could be too hydrophilic to cross the lipid bilayer efficiently and, as a consequence, the observed cellular uptake was hindered. The same conclusion was made by Sibrian-Vazquez et al. (2007) who synthesized a series of PEG-functionalized porphyrins and evaluated their *in vitro* biological properties. The authors noticed that the cellular uptake was dependent on the number of polymer chains linked to the porphyrin ring. It was found that tri- and four-substituted porphyrin with PEG chains were too hydrophilic as well as too aggregated to be efficiently delivered to the cells. In the case of p-THPP-PEG_{350} we observed the lowest efficiency of intracellular accumulation among all tested pegylated porphyrins. This effect can be explained by the low solubility of that compound and its tendency to aggregate in aqueous medium. Taking above into the consideration it can be concluded that the cellular accumulation of dyes was dependent on the PEG length, means of porphyrin delivery, cell line and incubation time.

3.3. Dark cytotoxicity and PDT efficacy measured with MTS assay

The dark toxicities of the pegylated porphyrins in solution and embedded into liposomes were investigated in both cell lines. The cells were exposed to increasing concentrations of each porphyrin system for 4 h and their viabilities were determined after 24 h using MTS assay. The results were presented in Table 2. As can be seen, all the studied formulations of p-THPP were non-toxic in the dark at the concentration up to 20 μg/mL. These findings are consistent with those reported in our previous paper (Nawalany et al., 2009), where it was shown that the dark cytotoxicity of p-THPP incorporated into SSL liposomes or modified by the covalent attachment of PEG chains is considerably reduced compared to the free photosensitizer. The lack of the dark toxicity of tetraarylporphyrins functionalized with 1-4 PEG chains was also demonstrated *in vitro* by Sibrian-Vazquez et al. (2007).

The reduction of HCT 116 and DU 145 cells viability after PDT with different photosensitizer systems was assessed using MTS assay. The values of the concentrations of the tested porphyrins systems leading to 50% inhibition of cell proliferation (IC_{50}) were determined and were collected in Table 2. Despite of some differences in viability of HCT 116 and DU 145 cell lines after PDT it is possible to compare the photosensitizing activities of the photosensitizers studied based on the values of IC_{50}. The free p-THPP is the most effective photosensitizer, with IC_{50} equal to 0.8 μg/mL (HCT 116) and 2.4 μg/mL (DU 145). However, that compound has considerable dark toxicity at the relatively low concentration. On the other hand, all the pegylated porphyrins exhibited very low dark cytotoxicities, but also lower than the parent compound phototoxicities. It was found that there was no simple correlation between efficiency of phototoxicity and length of PEG chain for the porphyrin-PEG conjugates. In the case of HCT 116, the highest efficiency was observed for p-THPP-PEG_{2000}, p-THPP-PEG_{5000} was less effective and the lowest efficiency was found for p-THPP-PEG_{350}. Whereas for the DU 145 cells it decreased in a series p-THPP-PEG_{2000} > p-THPP-PEG_{350} > p-THPP-PEG_{5000}.

Additionally, liposomal formulations of p-THPP-PEG_{2000} and p-THPP-PEG_{5000} required higher relative concentration of a porphyrin to achieve equitoxic effects to the photosensitizers delivered in PBS. This is particularly evident for the derivative with the longest PEG chain and DU 145 cells. It was observed that p-THPP-PEG_{5000} was non-phototoxic to the cells at the concentration up to 20 μg/mL. On the contrary, the incorporation of p-THPP-PEG_{350} into liposomes led to a significant improvement in the efficiency of PDT. In this case, the values of IC_{50} decreased by about two times for both cell lines studied. This may be related to poor solubility of p-THPP-PEG_{350} in water (Nawalany et al., 2008) and thus increased aggregation after its addition to the culture medium. Therefore, solubilization of this compound in liposomal bilayer greatly increases its bioavailability. This is strongly supported by uptake kinetics experiments (Fig. 3).

As can be seen in Table 2, all the examined systems showed higher photocytotoxicity against HCT 116 cells than against DU 145 cells. This finding is consistent with our previous observations that

Table 2
The values of IC_{50} for different systems (incubation time was 4 h) assessed against DU 145 and HCT 116 cells. MTS assay for the photo cytotoxicity was performed 24 h after irradiation.

Photosensitizing system	IC_{50} dark cytotoxicity (μg/mL)		IC_{50} photo cytotoxicity (μg/mL)	
	HCT 116	DU 145	HCT 116	DU 145
p-THPP in DMSO	5.4[a]	14[a]	0.8[a]	2.4[a]
p-THPP-PEG_{350} in DMSO	>20	>20	8.1	10.2
p-THPP-PEG_{2000} in PBS	>20	>20	2.6	3.76
p-THPP-PEG_{5000} in PBS	>20	>20	3.73	13.51
p-THPP in SSL liposomes	>50[a]	>50[a]	1.43[a]	>20[a]
p-THPP-PEG_{350} in liposomes	>20	>20	3.5	5.4
p-THPP-PEG_{2000} in liposomes	>20	>20	3.37	6.09
p-THPP-PEG_{5000} in liposomes	>20	>20	11.88	>20

[a] The values taken from Nawalany et al. (2009).

DU 145 cells are more resistant to PDT treatment than HCT 116 cells (Nawalany et al., 2009). However, the current study showed that p-THPP substituted with one PEG chain of molecular weight 2000 Da may have potential application in the treatment of prostate cancer.

Generally, p-THPP-PEG_{2000} was the most active among the tested derivatives both delivered in PBS or as incorporated into liposomes. Therefore, it was chosen for further detailed studies aiming to reveal the mechanism of these photosensitizers action.

3.4. Mechanism of cell death after PDT

The irradiation of cells incubated with photosensitizers altered cellular morphology as it was assessed under the inverted microscope. Fig. 2E and F shows as examples the morphology of HCT 116 cells after PDT sensitized with p-THPP-PEG_{2000} in PBS and enclosed in liposomes, respectively. The effects were dependent on the concentration of the photosensitizer. The population of cells was lower and their morphology changed dramatically; they were rounded and easily detaching from the bottom of the dish or they flattened while the cellular content was leaking out.

In the next step it was checked how rapidly the cell death occurs after PDT with different photosensitizer systems. We determined and compared the relative number of dead cells in both tested lines after 3, 6 and 24 h relapsed from PDT. The experiments were carried out at two different concentrations of the photosensitizers. These were established at the levels which ensured 60–80% and 90% (or higher) toxicity, respectively, in 24 h after PDT (for liposomal formulation the highest lethal effect observed in HCT 116 cells was 70% of dead cells at the concentration of photosensitizer as high as 20 μg/mL, and in DU 145 it was roughly 20% at the concentration

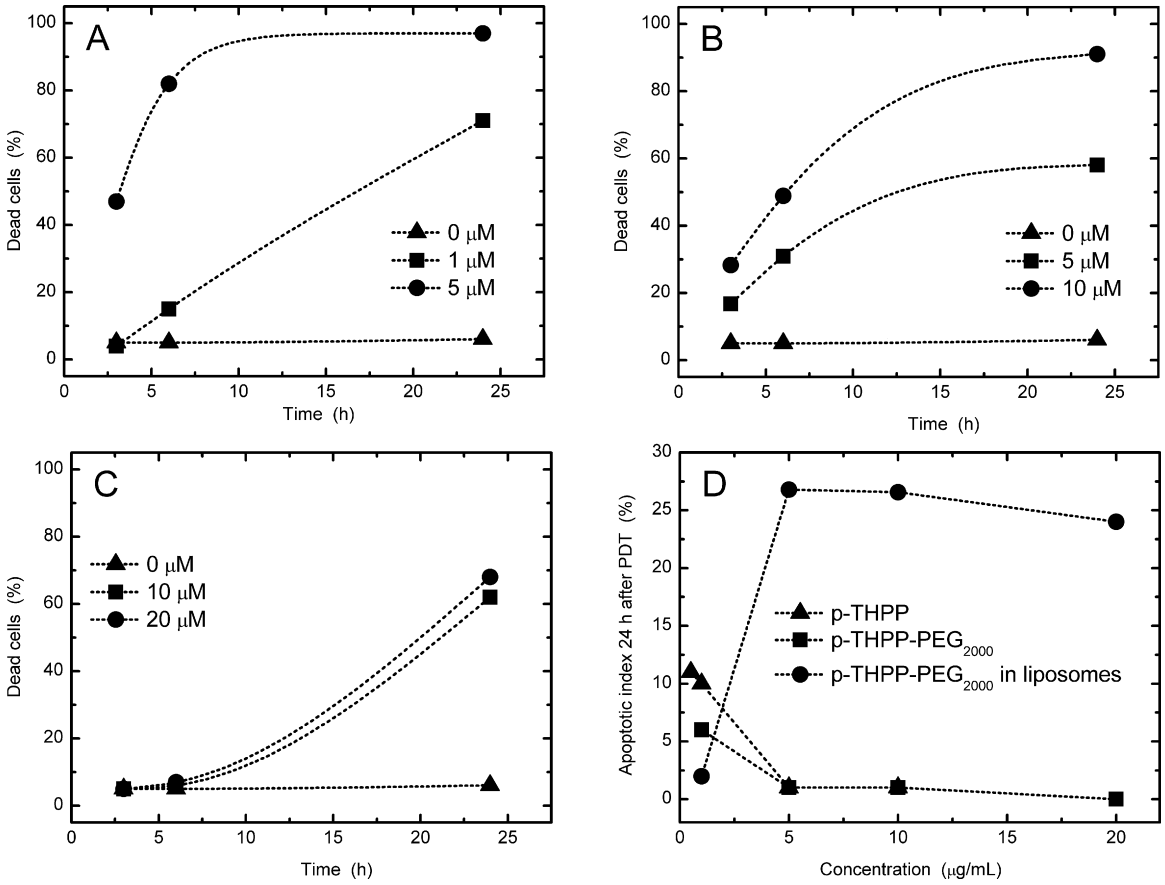

Fig. 4. (A–C) The percentage of dead HCT 116 cells after 3 h, 6 h and 24 h after PDT with p-THPP (A), p-THPP-PEG_{2000} (B) and p-THPP-PEG_{2000} in liposomes (C). The propidium iodide flow cytometric assay was used for the calculation of the percentage of dead cells. D – Apoptotic index counted 24 h after PDT with p-THPP, p-THPP-PEG_{2000} and p-THPP-PEG_{2000} in liposomes. The apoptotic cells were detected by DAPI staining and counted under fluorescence microscopy.

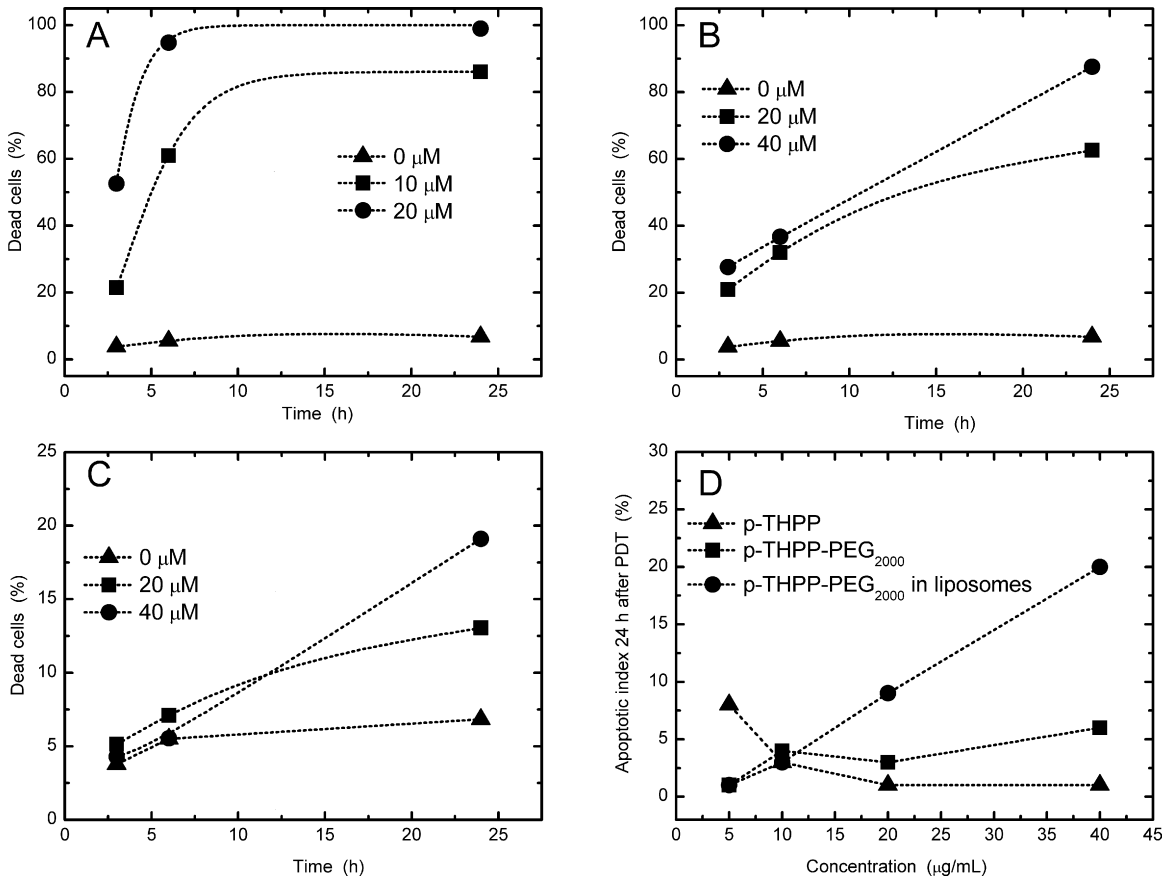

Fig. 5. (A–C) The percentage of dead DU 145 cells after 3 h, 6 h and 24 h after PDT with p-THPP (A), p-THPP-PEG_{2000} (B) and p-THPP-PEG_{2000} in liposomes (C). The propidium iodide flow cytometric assay was used for the calculation of the percentage of dead cells. D – Apoptotic index counted 24 h after PDT with p-THPP, p-THPP-PEG_{2000} and p-THPP-PEG_{2000} in liposomes. The apoptotic cells were detected by DAPI staining and counted under fluorescence microscopy.

of a photosensitizer of 40 μg/mL) (Figs. 4A–C and 5A–C). For the concentrations of p-THPP and p-THPP-PEG_{2000} leading to 90% or even higher toxicity, the number of dead cells in HCT 116 and DU 145 cell lines increased rapidly during first 6 h of incubation (Figs. 4A and B and 5A and B). When the photosensitizer was used at the concentration leading to 60–80% toxicity the number of dead cells in HCT 116 and DU 145 increased less rapidly during first 6 h after PDT. Interestingly, in the case when p-THPP-PEG_{2000} incorporated to liposomes was used, the number of dead cells observed up to 6 h after the irradiation increased only slightly above the level observed in the untreated control sample, so, in comparison with other photosensitizers used in the experiment, the cell death events were delayed. This suggested that cells treated with liposomal formulation of p-THPP-PEG_{2000} before irradiation might undergo slow apoptotic processes, which were very unlikely to be completed within that short (6 h) period of time after light exposure. In order to verify that hypothesis the cells were treated with increasing concentration of photosensitizers (Figs. 4D and 5D), irradiated and examined for nuclear signs of apoptosis in 24 h after treatment. Examples of nuclear morphology after PDT with porphyrins are presented in Fig. 2G–I.

The morphology of nuclei in DAPI stained specimens revealed condensation of DNA characteristic of apoptosis in 25% of HCT 116 cells and 20% of DU 145 cells after PDT with liposomal formulation of pegylated porphyrin at the concentration equal to or higher than IC_{50}. In the case of unmodified porphyrin, the apoptotic index did not exceed 12% at IC_{50} in HCT 116 cells and 9% in DU 145, and decreased with increasing concentration of p-THPP. It was reported that the cells treated with a higher PDT dose (a high concentration of the photosensitizer or/and dose of light) resulted in the necrotic cell death. On the contrary, at lower PDT doses the cells exhibited a greater ability to die in apoptotic manner (Mroz et al., 2011; Buytaert et al., 2007; Yoo et al., 2011; Nagata et al., 2003).

When p-THPP-PEG_{2000} in buffer solution was applied, the apoptosis was even less important; at IC_{50} apoptotic nuclei were observed only in 6% of HCT 116 cells and in 3% of DU 145 cells. Moreover, many cells showed nuclear swelling and DNA flocculation, characteristic of necrotic cells (Zhivotosky and Orrenius, 2001). Very low apoptotic index, necrotic structure of nuclei, together with fast death, occurring during 6 h after PDT suggest that cells treated with unmodified p-THPP or p-THPP-PEG_{2000} die mostly in a necrotic manner. We suppose that cells loaded with p-THPP or p-THPP modified with PEG of molecular weight 2000 Da suffer intense stress, whereas the cells treated with liposomal formulation of p-THPP-PEG_{2000} are less seriously affected, thus they can undergo and complete the process of active dying. It is a general phenomenon that, depending on the intensity of a stimulus, cells may die in necrotic or apoptotic manner (Formigli et al., 2000; Bonfoco et al., 1995; Shimizu et al., 1996). It seems likely that lethal injuries caused by different forms of photosensitizers used in our experiments that commit cells to die either by apoptosis or necrosis depend on the intensity of the stimulus which is the highest in case of unmodified porphyrin and the lowest in case of liposomal formulation of PEG_{2000}-modified p-THPP.

The results obtained from this study demonstrated that the photocytotoxicity of studied forms of p-THPP against both tested cell lines is mainly due to time-delayed effects appearing at different times post-irradiation. We have also observed that the concentration of the photosensitizer as well as their formulation have a major impact on time course of cell death occurring after PDT treatment.

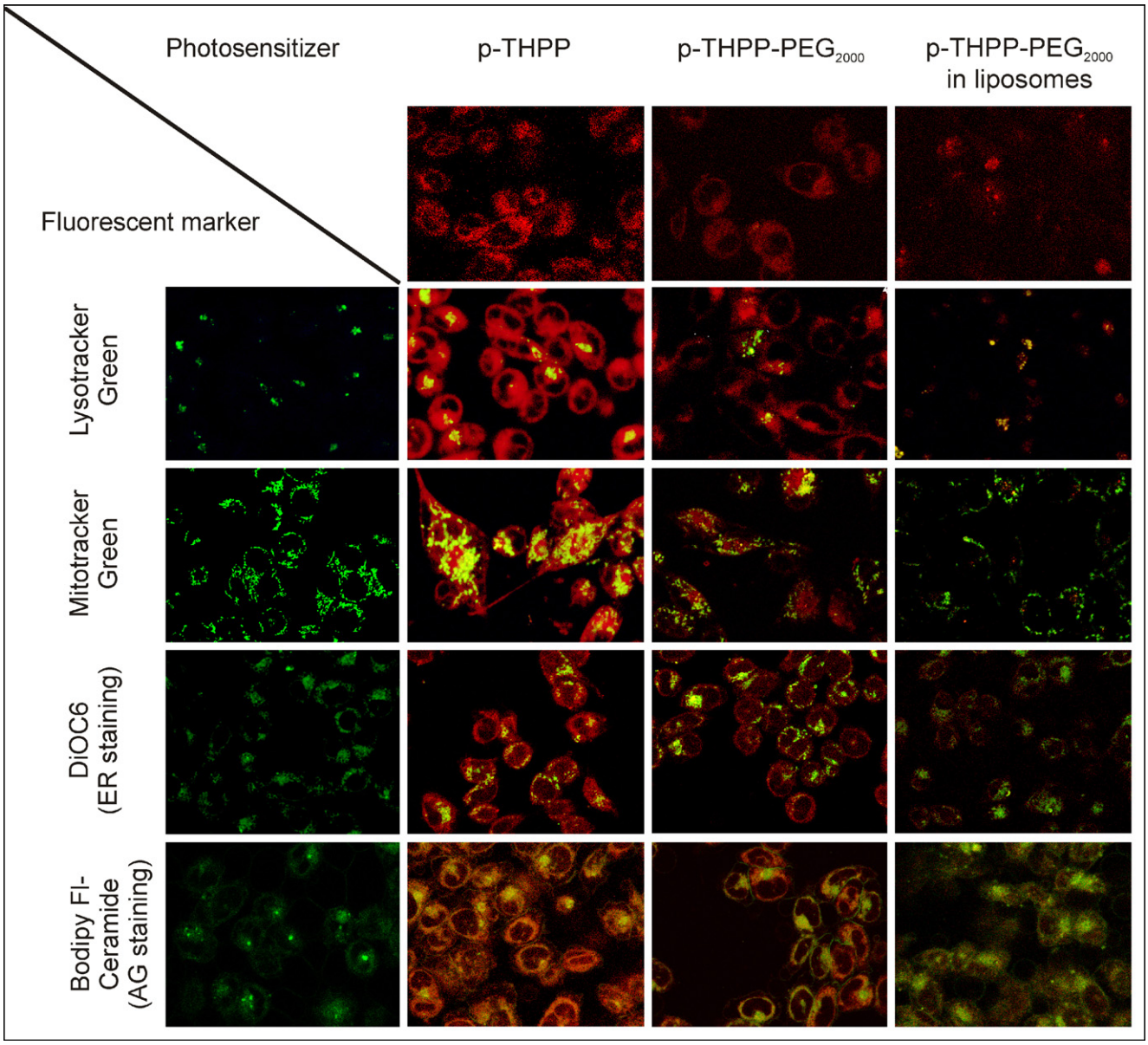

Fig. 6. HCT 116 cells treated for 4 h with porphyrins (p-THPP, p-THPP-PEG_{2000} and p-THPP-PEG_{2000} incorporated into liposomes) and then with fluorescent probes for lysosomes (Lysotracker Green), mitochondria (Mitotracker Green), endoplasmatic reticulum (DiOC6) and Golgi apparatus (Bodipy-Fl ceramide), as described in Section 2. Control cells were treated only with fluorescent probes (pictures in left column) or only with porphyrins (uppermost row). (For interpretation of the references to color in this figure legend, the reader is referred to the web version of the article.)

These finding are consistent with those reported by other authors. The influence of different parameters on the *in vitro* and *in vivo* efficacy of m-THPC was studied by Rezzoug et al. (1998). They showed that the phototoxicity of m-THPC was delayed and occurred 24 h after irradiation. This phenomenon was explained by the fact that the initial photochemical reactions induced by irradiation did not lead to cell photodamage.

3.5. *Intracellular localization of different formulations of porphyrins*

Preliminary observations on the cellular uptake of photosensitizers by HCT 116 and DU 145 cells suggested a rather non-specific intracellular distribution of p-THPP and its pegylated derivative when applied in the buffer. However, their liposomal formulations were concentrated mainly in vesicles in the vicinity of cell nucleus (Fig. 2B and C). It is commonly agreed, that the sub-cellular localization of photosensitizer determines the side and extent of the initial photodynamic damage and the cellular response to PDT (Oleinick et al., 2002; Goslinski and Piskorz, 2011). PDT mediated by a mitochondrion-targeting photosensitizer dissipates the mitochondrial membrane potential (Morgan and Oseroff, 2001), while alternatively, PDT with a lysosome-targeting photosensitizer causes the release of proteolytic lysosomal enzymes (Ichinose et al., 2006) and PDT with ER-targeted sensitizer causes ER stress and calcium release (He et al., 2010). The more thorough investigations of the diversity of subcellular localization of the porphyrin- and nonporphyrin-based photosensitizers are gathered in a few reviews (O'Connor et al., 2009; Castano et al., 2004; Buytaert et al., 2007; Sobolev et al., 2000).

There are many factors which influence on the localization of the photosensitizers, including structure and properties of the

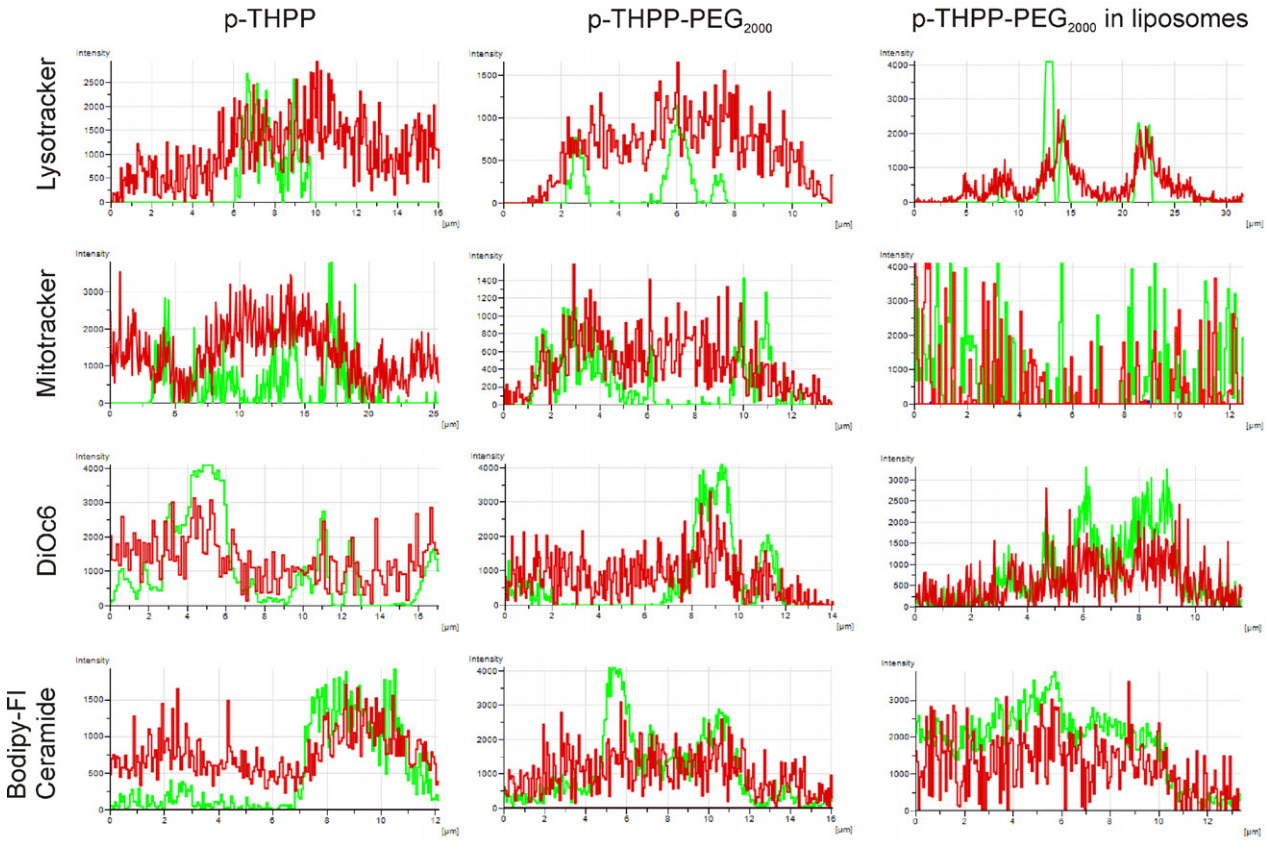

Fig. 7. Intensity profiles for red fluorescence (porphyrins) and green fluorescence (markers for organelles) along an axis crossing stained organelles in the representative HCT 116 cells. Cells were treated for 4 h with porphyrins (p-THPP, p-THPP-PEG_{2000} and p-THPP-PEG_{2000} incorporated into liposomes) and then with fluorescent probes for lysosomes (Lysotracker Green), mitochondria (Mitotracker Green), endoplasmatic reticulum (DiOC6) and Golgi apparatus (Bodipy-Fl ceramide), as described in Section 2. (For interpretation of the references to color in this figure legend, the reader is referred to the web version of the article.)

photosensitizer (hydrophobicity, charge distribution), means of delivery, mechanism of the cellular uptake and cell type (Takeuchi et al., 2004; Rancan et al., 2005; Jin and Zheng, 2011). We decided to compare intracellular localization of different photosensitizer systems in the HCT 116 cell line and to determine the correlation between the mode of cell death and pattern of intracellular distribution of photosensitizers.

The co-localization of the photosensitizer systems with fluorescent probes for subcellular structures is shown in Fig. 6. Nuclei appear to be free of any form of a photosensitizer. The free p-THPP and p-THPP-PEG_{2000} localize rather evenly in whole cellular volume, except for nucleus. In contrast, the pegylated porphyrin incorporated into liposomes exhibits preferential localization in lysosomes. A detailed analysis of spectral intensity profiles indicated also the presence of the studied photosensitizers in Golgi apparatus, in endoplasmatic reticulum and in mitochondria (Fig. 7).

In general, the liposomes are deliver to the cell interior by endocytosis or fusion mechanism (Batzri and Korn, 1975). As a result the photosensitizer enclosed in liposomes initially is accumulated in lysosomes but during or before irradiation it can be redistributed to the other organelles. In our studies the p-THPP-PEG_{2000} delivered in liposomes showed the preferential colocalization and strongest fluorescence signal in lysosomes, and the weakest in mitochondria. Although, the liposomes loaded with p-THPP-PEG_{2000} exhibited the lower photodynamic activity than the parent or pegylated porphyrin delivered in PBS (Figs. 4 and 5), it caused apoptosis on the highest level among tested photosensitizers (apoptotic index was 25% and 20% in HCT 116 and DU 145 cells, respectively). According to the literature, the lysosomal photosensitization induces apoptosis *via* two possible pathways: the relocation of the photosensitizers from lysosomes to other cellular targets, and the release of lysosomal enzyme, cathepsins, into the cytosol (Rancan et al., 2005; Reiners et al., 2002). Earlier studies (Rancan et al., 2005) on chlorines-based photosensitizers reveled that dyes can migrate within the cellular interior during incubation time. It was demonstrated that chlorins, which were primarily localized in the lysosomes, relocalized to the mitochondria and Golgi apparatus. Because of the fact that observed apoptosis response to PDT was delayed the authors concluded that apoptotic pathway was caused by the lysosomes photodamage rather than mitochondria. This explanation may account for observed results in our studies for liposomes loaded with p-THPP-PEG_{2000}. The delayed cell death response to PDT was also reported by Noodt et al. (1999). The authors observed different kinetics for the induction of apoptosis by irradiation of intracellular or lysosomes localized porphyrins. They found that photodamage to membranes resulted in immediate apoptosis, whereas in the case of PDT-induce damage to lysosomes the apoptotic cells did not appear until more than 12 h after irradiation.

Mitochondria-targeting photosensitizers are usually regarded as more efficient inducers of cell killing in comparison with the photosensitizers directed to endoplasmic reticulum or lysosomes. This is thought to stem from the observations that mitochondria-targeting photosensitizers directly induce apoptotic death (He et al., 2010). In the case of p-THPP and its pegylated form the dominant mechanism of PDT-initiated cell death was necrosis, despite the fact that the sensitizers appeared to be present also in mitochondria. Although the detailed determination of cell death mechanism is beyond the scope of current studies, we can speculate that ubiquitous distribution of the photosensitizer causes multiple effects in many important cellular targets during the irradiation,

which leads to the rapid necrotic death of the cell. It is worth noticing that the common observation that at low doses of damaging factor the cellular machinery for apoptosis is activated, whereas at higher doses, the apoptotic machinery is damaged and the cell undergoes rapid, necrotic death.

Our results indicate that encapsulation of p-THPP-PEG_{2000} in liposomes did not improve (or even weakened) the cytotoxic effect of PDT in comparison to application of pegylated porphyrins, due to slow intracellular accumulation of the photosensitizer. Thus, there is no need to use liposomes as carriers for pegylated porphyrins. Pegylation of a porphyrin with PEG of carefully chosen chain length could be a recommended solution allowing to prepare the photosensitizers with improved water solubility, low dark toxicity and high efficiency of PDT at relatively low concentrations.

4. Conclusions

Evaluation of the *in vitro* cytotoxicity of the series of PEG-functionalized porphyrins towards two cancer cell lines: HCT 116 and DU 145, revealed that the IC_{50} values of the tested compounds changes with the length of PEG chain in the drug-polymer conjugates. The most effective compound found in this assay was p-THPP-PEG_{2000} derivative, while the other polymer conjugates gave equitoxic effects at higher concentration. Liposomal formulation did not improve the uptake of that photosensitizer, and photocytotoxic effects with the use of that form of photosensitizer delivery system were weaker. The main difference in the effect of the application of a liposomal form of a photosensitizer and its buffer solution laid in a difference in their pattern of the intracellular distribution. That may further influence the mode of cell death after irradiation. Moreover, liposomal formulation of pegylated porphyrin resulted in a greater tendency to induce apoptotic cell death compared with the parent or pegylated m-THPP introduced in buffer. To sum up, pegylated p-THPPs, due to their good solubility in water, efficient accumulation in cytoplasm and photosensitizing properties, are promising candidates for drugs designed to be used in PDT therapy.

Acknowledgments

This project was operated within the Foundation for Polish Science Team Programme cofinanced by the EU European Regional Development Fund, PolyMed, TEAM/2008-2/6. The research was carried out with the equipment purchased thanks to the financial support of the European Regional Development Fund in the framework of the Polish Innovation Economy Operational Program (contract no. POIG.02.01.00-12-023/08).

References

Allison, R.R., Sibata, C.H., 2010. Oncologic photodynamic therapy photosensitizers: a clinical review. Photodiag. Photodyn. Ther. 7, 61–75.

Ball, D.J., Luo, Y., Kessel, D., Griffiths, J., Brown, S.B., Vernon, D.I., 1998. The induction of apoptosis by a positively charged methylene blue derivative. J. Photochem. Photobiol. B 42, 159–163.

Batzri, S., Korn, E.D., 1975. Interaction of phospholipid vesicles with cells. Endocytosis and fusion as alternate mechanisms for the uptake of lipid-soluble and water-soluble molecules. J. Cell Biol. 66, 621–634.

Berlanda, J., Kiesslich, T., Engelhardt, V., Krammer, B., Plaetzer, K., 2010. Comparative in vitro study on the characteristics of different photosensitizers employed in PDT. J. Photochem. Photobiol. B 100, 173–180.

Bonfoco, E., Krainc, D., Ankarcrona, M., Nicotera, P., Lipton, S.A., 1995. Apoptosis and necrosis: two distinct events induced, respectively, by mild and intense insults with N-methyl-D-aspartate or nitric oxide/superoxide in cortical cell cultures. Proc. Natl. Acad. Sci. U.S.A. 92, 7162–7166.

Bonnett, R., 1995. Photosensitizers of the porphyrin and phthalocyanine series for photodynamic therapy. Chem. Soc. Rev. 24, 19–33.

Bonnett, R., McGarvey, D.J., Harriman, A., Land, E.J., Truscott, T.G., Winfield, U.-J., 1988. Photophysical properties of meso-tetraphenylporphyrin and some meso-tetra(hydroxyphenyl)porphyrins. Photochem. Photobiol. 48, 271–276.

Buytaert, E., Dewaele, M., Agostinis, P., 2007. Molecular effectors of multiple cell death pathways initiated by photodynamic therapy. Biochim. Biophys. Acta 1776, 86–107.

Castano, A.P., Demidova, T.N., Hamblin, M.R., 2004. Mechanisms in photodynamic therapy: part one—photosensitizers, photochemistry and cellular localization. Photodiag. Photodyn. Ther. 1, 279–293.

Chen, B., Poque, B.W., Hasan, T., 2005. Liposomal delivery of photosensitising agents. Expert Opin. Drug Deliv. 2, 477–487.

Deda, D.K., Uchoa, A.F., Carita, E., Baptista, M.S., Toma, H.E., Araki, K., 2009. A new micro/nanoencapsulated porphyrin formulation for PDT treatment. Int. J. Pharm. 376, 76–83.

Dellinger, M., 1996. Apoptosis or necrosis following Photofrin photosensitization: influence of the incubation protocol. Photochem. Photobiol. 64, 182–187.

Derycke, A.S., de Wittle, P.A., 2004. Liposomes for photodynamic therapy. Adv. Drug Deliv. Rev. 56, 17–30.

Formigli, L., Papucci, L., Tani, A., Schiavone, N., Tempestini, A., Orlandini, G.E., Capaccioli, S., Zecchi Orlandini, S., 2000. Aponecrosis: morphological and biochemical exploration of a syncretic process of cell death sharing apoptosis and necrosis. J. Cell Physiol. 182, 41–49.

Goslinski, T., Piskorz, J., 2011. Fluorinated porphyrinoids and their biomedical applications. J. Photochem. Photobiol. C 12, 304–321.

Grahn, M.F., Giger, A., McGuinness, A., de Jode, M.L., Stewart, J.C.M., Ris, H.-B., Altermatt, H.J., Williams, N.S., 1999. mTHPP polymer conjugates: the in vivo photodynamic activity of four candidate compounds. Lasers Med. Sci. 14, 40–46.

Hamblin, M.R., Miller, J.L., Rizvi, I., Ortel, B., Maytin, E.V., Hasan, T., 2001. Pegylation of a chlorine6 polymer conjugate increases tumor targeting of photosensitizer. Cancer Res. 61, 7155–7162.

He, P., Ahn, J.C., Shin, J.I., Chung, P.S., 2010. Photoactivation of 9-hydroxypheophorbide alpha triggers apoptosis through the reactive oxygen species-mediated mitochondrial pathway and endoplasmic reticulum stress in AMC-HN-3 laryngeal cancer cells. Int. J. Oncol. 36, 801–808.

Henderson, B.W., Dougherty, T.J., 1992. How does photodynamic therapy work? Photochem. Photobiol. 55, 145–157.

Henderson, B.W., Beilnier, D.A., Greco, W.R., Sharma, A., Pandey, R.K., Vaughan, L.A., Weishaupt, K.R., Dougherty, T.J., 1997. An in vivo quantitative structure–activity relationship for a congeneric series of pyropheophorbide derivatives as photosensitizers for photodynamic therapy. Cancer Res. 57, 4000–4007.

Hornung, R., Fehr, M.K., Monti-Frayne, J., Krasieva, T.B., Tromberg, B.J., Berns, M.W., Tadir, Y., 1999. Highly selective targeting of ovarian cancer with the photosensitizer PEG-m-THPC in a rat model. Photochem. Photobiol. 70, 624–629.

Ichinose, S., Usuda, J., Hirata, T., Inoue, T., Ohtani, K., Maehara, S., Kubota, M., Imai, K., Tsunoda, Y., Kuroiwa, Y., Yamada, K., Tsutsui, H., Furukaw, K., Okunaka, T., Oleinick, N.L., Kato, H., 2006. Lysosomal cathepsin initiates apoptosis, which is regulated by photodamage to Bcl-2 at mitochondria in photodynamic therapy using a novel photosensitizer, ATX-s10 (Na). Int. J. Oncol. 29, 349–355.

Jin, C.S., Zheng, G., 2011. Liposomal nanostructures for photosensitizer delivery. Lasers Surg. Med. 43, 734–748.

Juzeniene, A., Peng, Q., Moan, J., 2007. Milestones in the development of photodynamic therapy and fluorescence diagnosis. Photochem. Photobiol. Sci. 6, 1234–1245.

Konan, Y.N., Berton, M., Gurny, R., Alleman, E., 2003a. Enhanced photodynamic activity of meso-tetra(4-hydroxyphenyl)porphyrin by incorporation into sub-200 nm nanoparticles. Eur. J. Pharm. Sci. 18, 241–249.

Konan, Y.N., Chevallier, J., Gurny, R., Alleman, E., 2003b. Encapsulation of p-THPP into nanoparticles: cellular uptake, subcellular localization and effect of serum on photodynamic activity. Photochem. Photobiol. 77, 638–644.

Lottner, Ch., Bart, K.-C., Bernhardt, H., Brunner, H., 2002. Soluble tetraarylporphyrin-platinum conjugates as cytotoxic and phototoxic antitumor agents. J. Med. Chem. 45, 2079–2089.

Moan, J., Peng, Q., 2003. An outline of the hundred-year history of PDT. Anticancer Res. 23, 3591–3600.

Mroz, P., Tegos, G.P., Gali, H., Wharton, T., Sarna, T., Hamblin, M.R., 2007. Photodynamic therapy with fullerenes. Photochem. Photobiol. Sci. 6, 1139–1149.

Mroz, P., Yaroslavsky, A., Kharkwal, G.B., Hamblin, M.R., 2011. Cell death pathways in photodynamic therapy of cancer. Cancer 3, 2516–2539.

Morgan, J., Oseroff, A.R., 2001. Mitochondria-based photodynamic anti-cancer therapy. Adv. Drug Delivery Rev. 49, 71–86.

Nagata, S., Obana, A., Gohto, Y., Nakajima, S., 2003. Necrotic and apoptotic cell death of human malignant melanoma cells following photodynamic therapy using an amphiphilic photosensitizer, ATX-S10(Na). Lasers Surg. Med. 33, 64–70.

Nawalany, K., Kozik, B., Kępczyński, M., Zapotoczny, S., Kumorek, M., Nowakowska, M., Jachimska, B., 2008. Properties of polyethylene glycol supported tetraarylporphyrin in aqueous solution and its interaction with liposomal membranes. J. Phys. Chem. B 112, 12231–12239.

Nawalany, K., Rusin, A., Kępczyński, M., Mikhailov, A., Kramer-Marek, G., Śnietura, M., Połtowicz, J., Krawczyk, Z., Nowakowska, M., 2009. Comparison of photodynamic efficacy of tetraarylporphyrin pegylated or encapsulated in liposomes: in vitro studies. J. Photochem. Photobiol. B 97, 8–17.

Noodt, B.B., Berg, K., Stokke, T., Peng, Q., Nesland, J.M., 1999. Different apoptotic pathways are induced from various intracellular sites by tetraphenylporphyrins and light. Br. J. Cancer 79, 72–81.

O'Connor, A.E., Gallagher, W.M., Byrne, A.T., 2009. Porphyrin and nonporphyrin photosensitizers in oncology: preclinical and clinical advances in photodynamic therapy. Photochem. Photobiol. 85, 1053–1074.

Oleinick, N.L., Moris, R.L., Belichenko, I., 2002. The role of apoptosis in response to photodynamic therapy: what, where, why, and how? Photochem. Photobiol. Sci. 1, 1–21.

Peng, C.L., Lai, P.S., Chang, C.C., Lou, P.J., Shied, M.J., 2010. The synthesis and photodynamic properties of meso-substituted, cationic porphyrin derivatives in HeLa cells. Dyes Pigments 84, 140–147.

Rancan, F., Wiehe, A., Nobel, M., Senge, M.O., Al Omari, S., Bohm, F., John, M., Roder, B., 2005. Influence of substitutions on asymmetric dihydroxychlorins with regard to intracellular uptake, subcellular localization and photosensitization of Jurkat cells. J. Photochem. Photobiol. B 78, 17–28.

Reiners Jr., J.J., Caruso, J.A., Mathieu, P., Chelladurai, B., Yin, X.M., Kessel, D., 2002. Release of cytochrome c and activation of pro-caspase-9 following lysosomal photodamage involves bid cleavage. Cell Death Differ. 9, 934–944.

Rezzoug, H., Bezdetnaya, L., A'amar, O., Merlin, J.L., Guillemin, F., 1998. Parameters affecting photodynamic activity of Foscan® or meta-tetra(hydroxyphenyl)chlorine (mTHPC) in vitro and in vivo. Lasers Med. Sci. 13, 119–125.

Roberts, M.J., Bentley, M.D., Harris, J.M., 2002. Chemistry for peptide and protein PEGylation. Adv. Drug Delivery Rev. 54, 459–476.

Roslaniec, M., Weitman, H., Holmes, R.T., Smith, K.M., Ehrenberg, B., 2000. Liposome binding constants and singlet oxygen quantum yields of hypericin, tetrahydroxy helianthrone and their derivatives: studies in organic solutions and in liposomes. J. Photochem. Photobiol. B 57, 149–158.

Roy, I., Ohulchanskyy, T.Y., Pudavar, H.E., Bergey, E.J., Oseroff, A.R., Morgan, J., Dougherty, T.J., Prasad, P.N., 2003. Ceramic-based nanoparticles entrapping water-insoluble photosensitizing anticancer drugs: a novel drug-carrier system for photodynamic therapy. J. Am. Chem. Soc. 125, 7860–7865.

Shimizu, S., Eguchi, Y., Kamiike, W., Itoh, Y., Hasegawa, J., Yamabe, K., Otsuki, Y., Matsuda, H., Tsujimoto, Y., 1996. Induction of apoptosis as well as necrosis by hypoxia and predominant prevention of apoptosis by Bcl-2 and Bcl-XL. Cancer Res. 56, 2161–21663.

Sibrian-Vazquez, M., Jensen, T.J., Vicente, M.G.H., 2007. Synthesis and cellular studies of PEG-functionalized meso-tetraphenylporphyrins. J. Photochem. Photobiol. B 86, 9–21.

Sobolev, A.S., Jans, D.A., Rosenkranz, A.A., 2000. Targeted intracellular delivery of photosensitizers. Prog. Biophys. Mol. Biol. 73, 51–90.

Takeuchi, Y., Ichikawa, K., Yonezawa, S., Kurowane, K., Koishi, T., Nango, M., Namba, Y., Oku, N., 2004. Intracellular target for photosensitization in cancer antiangiogenic photodynamic therapy mediated by polycation liposome. J. Control. Rel. 97, 231–240.

Vargas, A., Pegaz, B., Debefve, E., Konan-Kouakou, Y., Lange, N., Ballini, J-P., Van den Bergh, H., Gurny, R., Delie, F., 2004. Improved photodynamic activity of porphyrin loaded into nanoparticles: an in vivo evaluation using chick embryos. Int. J. Pharm. 286, 131–145.

Westermann, P., Glanzmann, T., Andrejevic, S., Braichotte, D.R., Forrer, M., Wagnieres, G.A., Monnier, P., van den Bergh, H., Mach, J.-P., Folli, S., 1998. Long circulating half-life and high tumor selectivity of the photosensitizer meta-tetrahydroxyphenylchlorin conjugated to polyethylene glycol in nude mice grafted with a human colon carcinoma. Int. J. Cancer 76, 842–850.

Wyld, L., Reed, M.W.R., Brown, N.J., 2001. Differential cell death response to photodynamic therapy is dependent on dose and cell type. Br. J. Cancer 84, 1384–1386.

Yoo, J.-O., Lim, Y.-C., Kim, Y.-M., Ha, K.-S., 2011. Differential cytotoxic responses to low- and high-dose photodynamic therapy in human gastric and bladder cancer cells. J. Cell. Biochem. 112, 3061–3071.

Zhao, B., Yin, J.-J., Bilski, P.J., Chignell, C.F., Roberts, J.E., He, Y.-Y., 2009. Enhanced photodynamic efficacy towards melanoma cells by encapsulation of Pc4 in silica nanoparticles. Toxicol. Appl. Pharmacol. 241, 163–172.

Zhivotosky, B., Orrenius, S., 2001. Assessment of apoptosis and necrosis by DNA fragmentation and morphological criteria. Curr. Protoc. Cell Biol. (Chapter 18: Unit 18.3).